Synthesis and Characterization of Molecular Composite Prepared from Layered Perovskite Oxide, $HLa_2Ti_2NbO_{10}$

Young-Sik Hong and Si-Joong Kim

Department of Chemistry, Korea University, Seoul 136-701, Korea
Received March 11, 1997

A layered perovskite oxide, $RbLa_2Ti_2NbO_{10}$, was prepared and investigated for proton exchange and intercalation behaviors. Its protonated form, $HLa_2Ti_2NbO_{10}$, exhibits the Brønsted acidity and reacts with organic amines. Polyoxonuclear cation, Al_{13}, was then introduced into the interlayer by refluxing octylamine-intercalated compound with an Al_{13} pillaring solution. These layered oxides were characterized by X-ray diffractometer, thermogravimeter, FT-infrared spectrometer and elemental analyzer. It is observed that the polyoxonuclear cation-pillared material exhibits a bilayer structure and is thermally more stable than organic counterpart at higher temperatures. The surface area of the pillared material annealed at 400 °C was the value of 25.1 m^2/g.

Introduction

Since the discovery of zeolites as a fluid-cracking catalyst, many alternatives, such as clay minerals, phosphates and layered oxides, have been extensively synthesized to exploit the selectivity differences possible with different pore geometries and catalyst compositions.[1-8] It has been shown that the microporous materials with various pores can be constructed by incorporating inorganic pillars between the two layers of layered oxides. However, these pillaring procedures are not applicable to some layered oxides because the layers are not readily opened up to introduce pillars. Therefore, new synthetic approaches have been created by utilizing organically preswelled intercalation compounds, which facilitate the replacement by a large polyoxonuclear cation such as $Al_{13}O_4(OH)_{24}(H_2O)_{12}^{7+}$ (Al_{13}) having Keggin ion structure.[4] There is an obvious interest as a route to develope the pillared materials with specific properties.

In 1981, Dion *et al.* synthesized a new family of the layered oxides, $MCa_2Nb_3O_{10}$ with the general formula of $MA_{n-1}B_nO_{3n+1}$, where M and $A_{n-1}B_nO_{3n+1}$ indicate interlayer alkali metal and perovskite structured layer, respectively.[9] Subsequently, other related oxides such as $KCa_2Na_{n-3}Nb_nO_{3n+1}$, $K_{1-x}La_xCa_{2-x}Nb_3O_{10}$, $MPb_2Nb_3O_{10}$, $MCa_2Nb_{3-x}Al_xO_{10-x}$ and $MCa_2Nb_{3-x}Fe_xO_{10-x}$, $MCa_{2-x}La_xNb_{3-x}Ti_xO_{10}$ and $KSr_2Nb_3O_{10}$ have been also described and recently dubbed the Dion-Jacobson phases.[10-14] These oxides have a lower layer charge than the Ruddlesden-Popper phases of $M_2A_{n-1}B_nO_{3n+1}$ and, therefore, can be transformed into protonated forms, which can react further with organic bases by acid-base reaction.

Recently, the pillaring of Al_{13} have been tried to develope porous materials, based on the layered oxide, $KCa_2Nb_3O_{10}$.[15,16] However, its structure has been identified as the stuffed form composed of pillars and perovskite layers, because of high layer charge. Mohan Ram and Clearfield proposed new strategies for producing porous materials based on the Dion-Jacobson phases as follows: 1) partial intercalation of Al_{13}, 2) further reduction of the layer charge and 3) use of narrower pillars.[15]

Among them, the partial intercalation of Al_{13} may be achieved by the layered oxide, $RbLa_2Ti_2NbO_{10}$ (RbLTN), which was first prepared by Gopalakrishnan *et al.*[13] Its protonated phase, $HLa_2Ti_2NbO_{10}\cdot 1.5H_2O$, was proposed to a weak acid hardly intercalating organic bases due to the ordering of titanium and niobium in perovskite layers. In the present study, we have synthesized organic amine-intercalated compounds using the protonated phase of RbLTN and then obtained a Al_{13}-pillared material (Al_{13}-PM) by the incorporation of Al_{13}. In addition, the thermal stabilities and the surface areas of Al_{13}-PM and organic counterpart were compared with each other.

Experimental

Preparation. The compound RbLTN was prepared by firing stoichiometric amounts of Rb_2CO_3, La_2O_3, TiO_2 and Nb_2O_5 at 1150 °C in air for 2 days. An excess of Rb_2CO_3 (25 mol%) was added to compensate for the loss due to the volatilization of the rubidium component. Ten grams of RbLTN was converted to a protonated form, HLTN, by refluxing with aqueous 4 N HCl solution at 60 °C for 4 days, with acid being replaced everyday. Organic amine-intercalated compounds were prepared by refluxing the HLTN with 10% alkylamine and alkyldiamine in water or heptane for 3 days at 60-90 °C. After that, the products were centrifuged, decanted, washed and dried under vacuum.

A pillaring solution was prepared by slowly adding 0.4 N NaOH to 0.4 N $AlCl_3$ with vigorous stirring as reported previously.[14] The Al_{13} in pillaring solution was checked by ^{27}Al NMR spectrum using a $[Al(H_2O)_6]^{3+}$ as an external reference. As NaOH is added a sharp line appears at 62.8 ppm. Akitt *et al.* have assigned that the peak is attributed to the tetrahedral aluminum of Al_{13}.[17] The octylamine-intercalated compound of 600 mg was reacted with a 50 mL portion of the pillaring solution (23.5 mmol Al^{3+}) for 2 days.

Characterization. The characterization of the layered oxides was conducted by powder X-ray diffractometer (XRD, Rigaku D-MAX III-b), FT-infrared spectrometer (FT-IR, BOMEN MB-102), thermogravimeter (TGA, STANTON RED CROFT TGA-1000), elemental analyzer (EA,

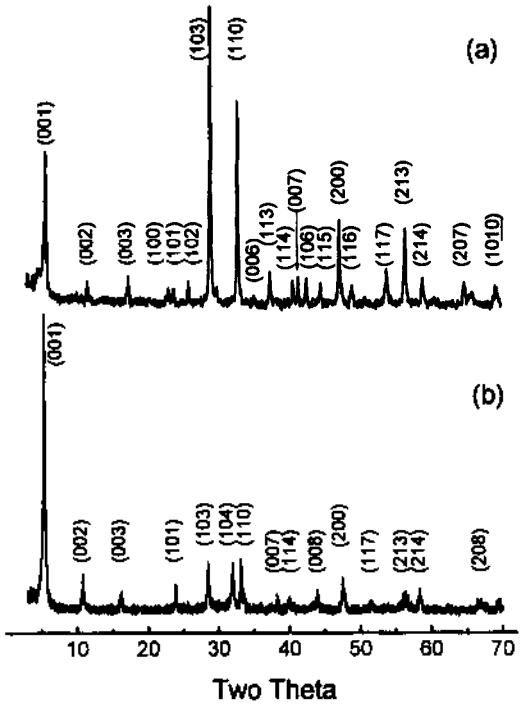

Figure 1. X-ray diffraction patterns of layered oxides. (a) $RbLa_2Ti_2NbO_{10}$ and (b) its protonated form.

CARLO ERBA EA 1108) and energy-dispersive X-ray spectrometer (EDS, JEOL JSM-35F). BET surface areas were measured on a Quantachrome Autosorb-6 automated surface analysis instrument.

Results and Discussion

Structural analysis of $RbLa_2Ti_2NbO_{10}$ and its protonated form. Figure 1 shows the powder XRD patterns of RbLTN and HLTN. In RbLTN all the reflections could be indexed in tetragonal structure with the lattice parameter of a=3.834 Å and c=15.240 Å. This indicates a half basal spacing of corresponding $KCa_2Nb_3O_{10}$, which crystallizes in an orthorhombic structure as listed in Table 1. The difference of basal spacing between the two layered oxides is in the way that the interlayer ions such as rubidium or potassium occupy the interlayer sites. The larger size of rubidium ion leads to an eclipsed arrangement of adjacent perovskite layers, stacked with one directly above the next, to give an 8-fold coordination resulting in a half c axis as shown in Figure 2. Unlike this, in $KCa_2Nb_3O_{10}$, perovskite layers are staggered by a/2 translation to give a 6-fold coordinated potassium ions. The basal spacing of HLTN is similar with those of RbLTN and $HCa_2Nb_3O_{10}\cdot 1.3H_2O$ due to large interlayer hydroxonium ion, H_3O^+, likewise rubidium ion. Typical elemental analysis of HLTN revealed that the replacement of Rb^+ by proton had proceeded above 95%. TG experiment also confirms that HLTN can be formulated as $HLa_2Ti_2NbO_{10}\cdot 1.3H_2O$.

Table 1. Lattice parameters of $RbLa_2Ti_2NbO_{10}$ and its protonated phases

Designation	Composition	a (Å)	b (Å)	c (Å)
RbLTN	$RbLa_2Ti_2NbO_{10}$	3.834		15.240
RbLTN[†]	$RbLa_2Ti_2NbO_{10}$	3.833		15.240
KCN[†]	$KCa_2Nb_3O_{10}$	3.853	3.868	29.470
HLTN	$HLa_2Ti_2NbO_{10}\cdot 1.3H_2O$	3.828		16.462
HLTN[†]	$HLa_2Ti_2NbO_{10}\cdot 1.5H_2O$	3.831		16.440
HCN[†]	$HCa_2Nb_3O_{10}\cdot 1.3H_2O$	3.849		16.210

[†,‡]: from reference 13 and 9, respectively

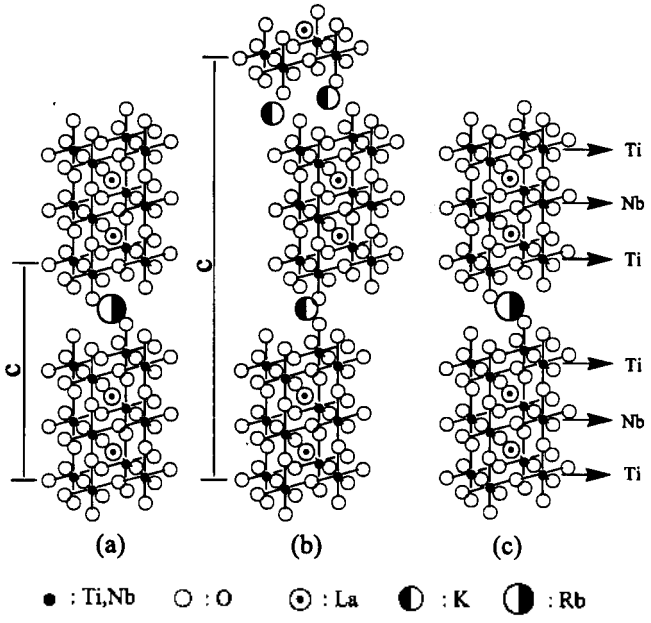

Figure 2. Schematic structures of layered oxides. (a) disordered $RbLa_2Ti_2NbO_{10}$, (b) $KCa_2Nb_3O_{10}$ and (c) ordered $RbLa_2Ti_2NbO_{10}$.

The synthesis of layered oxides of $MLa_2Ti_2NbO_{10}$ (M=Na, K, Rb and Cs) strongly depended on the size of interlayer ions. For M=Rb and Cs, the layered oxides were successfully obtained, but potassium analog was consisted of a mixed phase of layered oxide, $KLa_2Ti_2NbO_{10}$, and unknown phase, and sodium analog was not synthesized at all. In addition, we have tried to synthesize a new series of $Rb_{1-x}La_2Ti_{2-x}Nb_{1+x}O_{10}$ (x=0.2, 0.4, 0.6 and 0.8) oxides to obtain layered oxides with low layer charge by modifying the composition of B-site cation. However, single-phase layered oxides were not obtained because of the impurity phases like $La_4Ti_9O_{24}$ (JCPDS No. 15-324), amount of which was increased with decreasing rubidium content.

Intercalation reaction. The protonated phase, HLTN, was reacted with organic bases such as alkylamines and alkyldiamines. Figure 3 shows the XRD patterns of organic amine-intercalated compounds, which exhibit the large shift of (001) peak indicating the change of basal spacing. These are absolutely contrast to the result of Gopalakrishnan *et al.* [13] They did not observe an intercalation reaction in HLTN and explained as follows: the NbO_6 octahedra in perovskite layers are in the middle position flanked by the two TiO_6 octahedra, as shown in Figure 2(c), and then the interlayer protons are attached to the TiO_6 octahedra. This leads to the lower acidity due to lower oxidation state of titanium than that of niobium, as is supported by the acidity order of $HNb_3O_8\cdot H_2O$ > $HTiNbO_5$ > $H_2Ti_4O_9$. That is, HLTN can not intercalate organic bases due to lower acidity of Ti-O-H

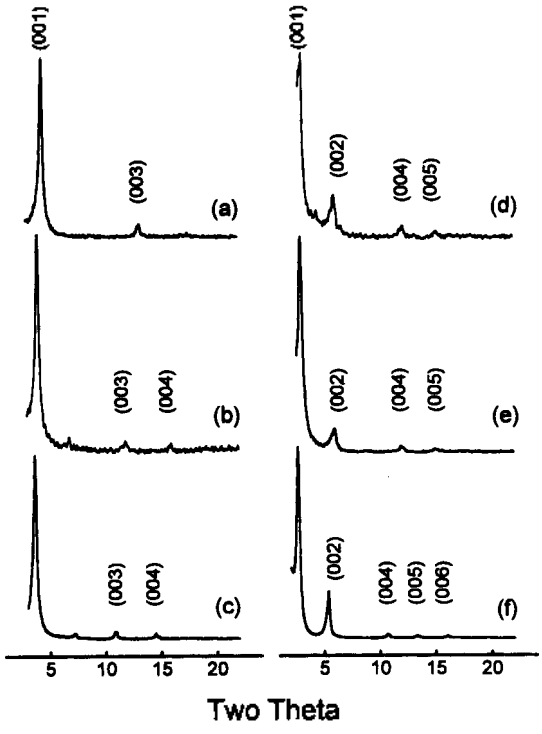

Figure 3. X-ray diffraction patterns of organic amine-intercalated compounds of (a) butyldiamine, (b) hexyldiamine, (c) octyldiamine, (d) butylamine, (e) hexylamine and (f) octylamine.

than that of Nb-O-H.[18,19]

However, many organic amines with pK_a>9 have been intercalated into $H_2Ti_4O_9$, even weak bases with pK_a>6 can intercalate into $HTiNbO_5$.[18] In addition, as is noted by them, it is well known that B' and B" ions in perovskite structured $A(B'_{1/3}B''_{2/3})O_3$ compounds can be ordered when there are significant differences in their size and charge.[20] The sizes of Nb^{5+} (0.64 Å) are nearly the same with that of Ti^{4+} (0.605 Å) and their charge difference is only one. Therefore, the explanation that intercalation reaction cannot occur because of the lowered acidity of Ti-O-H due to ordering of niobium and titanium, is not reasonable to this system. HLTN can act as solid Brønsted acid as well as $HTiNbO_5$ and react with organic amines such as alkylamines with pK_a~10.6 to give organic ammonium ions as follows: $xRNH_2$+HLTN→$(RNH_3)_xH_{1-x}LTN$ or xH_2NRNH_2+HLTN→$(H_3NRNH_3)_xH_{1-2x}LTN$.[21] The difference of reactivity may be ascribed to the reaction conditions. The refined unit cell parameters and intercalated organic contents for organic amine-intercalated compounds are listed in Table 2. For alkyldiamine-intercalated compounds, the organic content is rather larger than stoichiometric content. This may be considered as neutral alkyldiamines flanked between the alkyldiammonium ions.

Spatial arrangement of organic ammonium ions. Figure 4 shows the expansion of basal spacing for the alkylamine-intercalated compounds, (1), and alkyldiamine-intercalated compounds, (2), indicating the formation of bilayer and monolayer structures, respectively. Least squares fits of the data for the two types give the following lines:

$$c=1.924\ n+17.916\ \text{Å for (1) } \alpha=49.2°$$

Table 2. Lattice parameters and intercalated amine contents of the organic amine-intercalated compounds

Composition	a (Å)	c (Å)
$[CH_3(CH_2)_3NH_3]_{0.90}H_{0.10}La_2Ti_2NbO_{10}$	3.828	25.606
$[CH_3(CH_2)_5NH_3]_{0.90}H_{0.10}La_2Ti_2NbO_{10}$	3.833	29.466
$[CH_3(CH_2)_7NH_3]_{0.87}H_{0.13}La_2Ti_2NbO_{10}$	3.834	33.300
$[NH_3(CH_2)_4NH_3]_{0.50}La_2Ti_2NbO_{10}$	3.840	20.284
$[NH_3(CH_2)_6NH_3]_{0.50}[NH_2(CH_2)_6NH_2]_{0.07}La_2Ti_2NbO_{10}$	3.835	22.342
$[NH_3(CH_2)_8NH_3]_{0.50}[NH_2(CH_2)_8NH_2]_{0.09}La_2Ti_2NbO_{10}$	3.819	24.563

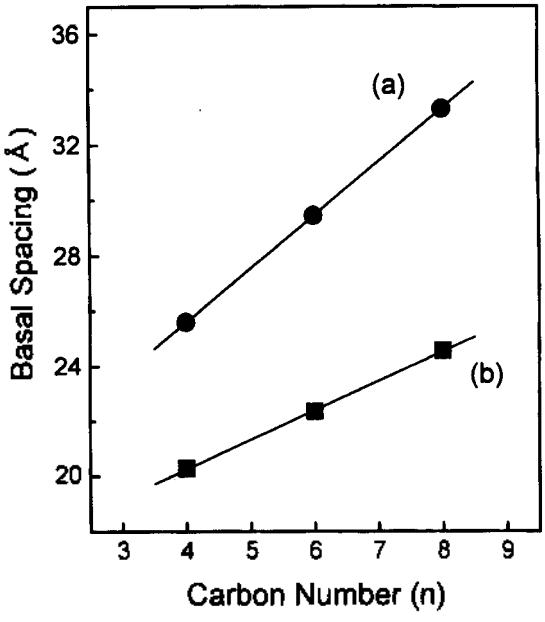

Figure 4. Basal spacing of (a) alkylamine- and (b) alkyldiamine-intercalated compounds.

$$c=1.070\ n+15.978\ \text{Å for (2) } \alpha=57.4°,$$

where c and n indicate the c axis spacing and the carbon number, respectively. Assuming the methylene groups in alkyl chain would have all trans conformations, the chain length grows by 1.27 Å per an added methylene group. For (1) and (2), the inclination angles (α) of the alkyl chain to the basal plane are different each other.

According to the result of Jacobson *et al.*, intercalation compounds based on $HCa_2Nb_3O_{10}$ have been divided into four distinct groups (I~IV), depending on the relative strength between van der Waals interaction of alkyl chains and hydrogen bond of the ammonium head group and the oxygen atom of layer surface.[22] In (1), the inclination angle is similar to the group II (α=56.5°). In (2), the inclination angle is in the middle of group II and group III (α=40.5°). It can be concluded, therefore, that the strength of hydrogen bonding in (2) is stronger than van der Waals interaction because of the presence of two active binding sites in diamines. On the other hand, in (1) the bilayer structure is stabilized by the increase of van der Waals interaction by increasing contact area between the alkyl chains.

Pillaring of polyoxoaluminate ion, Al_{13}. The mainshortcomings of organic amine-intercalated compounds are their insufficient thermal stability for application as ca-

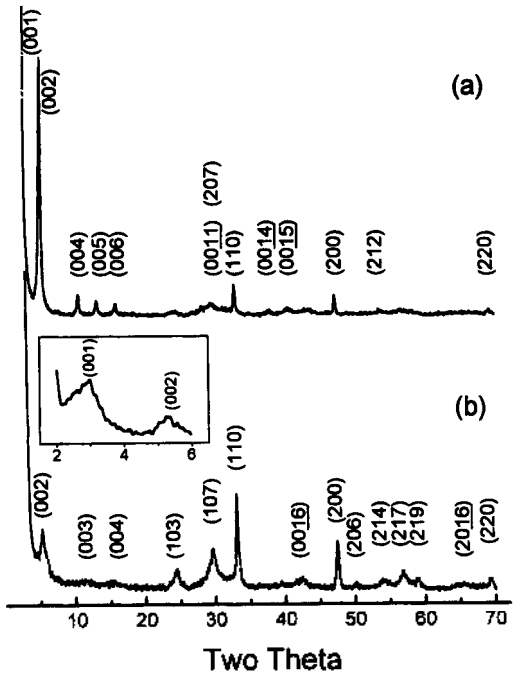

Figure 5. X-ray diffraction patterns of (a) OALTN (b) Al_{13}-PM.

talysts in high-temperature process. Accordingly, a pillaring has been undertaken to develop a thermostable porous material by introduction of Al_{13} pillar.[23] Figure 5 shows the XRD patterns of octylamine-intercalated compound (OALTN) and Al_{13}-PM. While the spacing of the (00l) reflections varied, the peaks corresponding to (110) and (200) reflections remain unchanged suggesting that the perovskite layers are robust and intact during the pillaring reaction. The broad reflections in Al_{13}-PM may be ascribed to some disorder in Al_{13} arrangements or incorporation of lower charged species with Al_{13} in the interlayer space, resulting in stresses on the layers.

The basal spacing of Al_{13}-PM, 34.1 Å, indicates a double layer of Al_{13}, diameter of which is in the range of 8.6-11.0 Å. The thickness of $La_2Ti_2NbO_{10}^-$ layers can be estimated by subtracting the diameter of 8-fold Rb^+ ion (3.22 Å) from the interlayer distance of RbLTN (15.240 Å), and a value of 12.02 Å is obtained. It is concluded, from the calculated basal spacing of *ca.* 29.2-33.0 Å for bilayer arrangement, that the arrangement of Al_{13} in Al_{13}-PM is a bilayer.[15]

FT-IR study. The FT-IR spectra of RbLTN, HLTN, OALTN and Al_{13}-PM provide the informations on the nature of interlayer ions. (Figure 6). The broad bands at 750-500 cm $^{-1}$, assigned to metal-oxygen stretching vibrations were not nearly varied. However, the band at 939 cm^{-1} in RbLTN changed successively to 962, 951 and 993, and 950 cm $^{-1}$ for HLTN, OALTN, and Al_{13}-PM, respectively. The peak at 962 cm^{-1} in HLTN disappeared after thermal treatment at 700 °C, indicating the bending modes of interlayer ions. In addition, a pair of strong bands in 2911 and 2845 cm $^{-1}$ at OALTN can be assigned to the methylene group. As the organic amines incorporated into the layer, the N-H bending mode of ammonium group due to acid-base reaction appeared at 1610-1530 cm^{-1}, which disappeared by a substitution of Al_{13}.

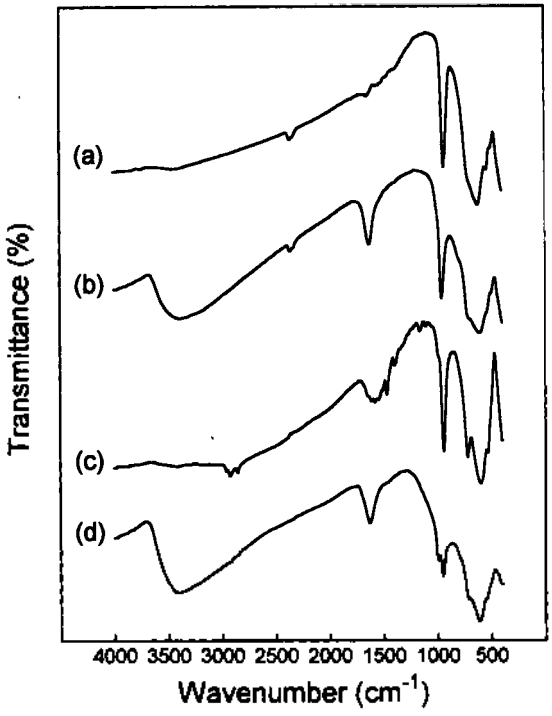

Figure 6. FT-IR spectra of (a) RbLTN, (b) HLTN, (c) OALTN and (c) Al_{13}-PM.

Thermal Stability of OALTN and Al_{13}-PM. Calcining of OALTN and Al_{13}-PM were conducted to investigate for the thermal behavior. Figure 7 shows the XRD

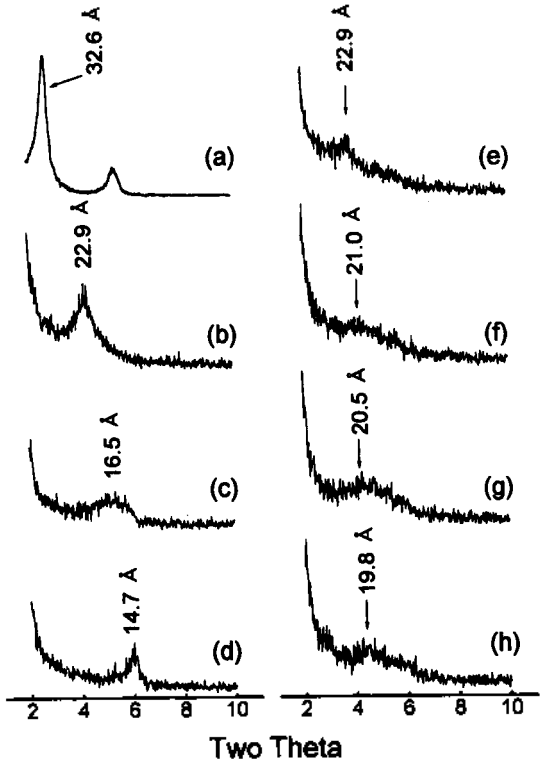

Figure 7. X-ray diffraction patterns of OALTN calcined at (a) 200, (b) 300, (c) 400 °C for 10 min and annealed at (d) 400 °C for 1 h, and Al_{13}-PM calcined at (e) 200, (f) 300, (g) 400 °C for 10 min and annealed at (h) 400 °C for 1 h, respectively.

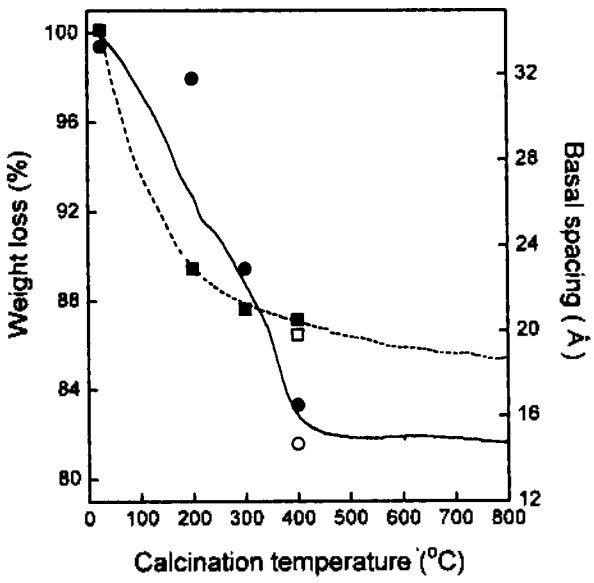

Figure 8. TG curves (—, ···) and the changes of basal spacing (symbols) of OALTN and Al_{13}-PM with calcination temperature at a heating rate of 10 °C/min. (●, ■: calcined for 10 mim; ○, □: annealed for 1 h)

patterns of OALTN and Al_{13}-PM calcined at various temperatures. The changes of basal spacing are plotted with TG curves (Figure 8). TG analysis of Al_{13}-PM shows that decomposition proceeds in two stages: dehydration begins just above room temperature and reaches a plateau above 500 °C. This is very close relation to the result of XRD. In Al_{13}-PM the large weight loss on calcination was accompanied by an initial rapid contraction of the interlayer spacing from 34.1 Å to 22.9 Å after heat treatment at 200 °C. Further heating levelled off the basal spacing to *ca.* 20.0 Å. This is good agreement with the result of Hardin *et al.*[15] The Al_{13} pillars have been completely condensated to give an alumina pillars according to the following reaction, $[Al_{13}O_4(OH)_{24}(H_2O)_{12}]^{7+} \rightarrow 6.5Al_2O_3 + 7H^+$.[6] Upon heating, the protons are released, and they in part balance the negative charge of the host layers, thereby producing coordinatively unsaturated Lewis acid sites in alumina and Brønsted acid sites in host layers to impart chemical catalytic properties.[6,24] On the other hand, the corresponding basal spacing of OALTN initially remained constant in value but abruptly decreased as organic components were decomposed above 300 °C.

The chemical composition of Al_{13}-PM was determined by TGA and EDS analysis. Assuming that the composition of Al_{13}-PM to $(Al_{13})_xLTN \cdot yH_2O$, the value of x, calculated from aluminum content using EDS based on the relative ratio of aluminum to niobium, is 0.09. In Al_{13}-PM the content of hydrated water was calculated from the weight loss of interlamellar water and the water bonded to aluminum in TG, over a temperature range of 25-300 °C. After pillaring of Al_{13}, residual octylammonium ion was not almost detected by FT-IR and EA. Then, Al_{13}-PM can be formulated as $(Al_{13})_{0.09}[CH_3(CH_2)_7NH_3]_{0.24}H_{0.13}LTN \cdot 6.7H_2O$. The observed aluminum content is smaller than that expected from the layer charge (1/7=0.14). This may be critically important to the synthesis of porous nanocomposites. Clearfield *et al.* and Hardin *et al.* have reported the $KCa_2Nb_3O_{10}$-based nanocomposites with no large increase in surface area due to the stuffed structure, resulted from a large amount of Al_{13}.[15,16] The surface area of the Al_{13}-PM annealed at 400 °C for 1 h was the value of 25.1 m^2/g, which was rather higher than that of the $KCa_2Nb_3O_{10}$-based materials, ~5 m^2/g. However, we have not certainly determined whether the increase of surface area of Al_{13}-PM may be from a porous structure or a small particle size. And the surface area is still small for pillared materials.

In summary, we have successfully prepared the organic amine-intercalated compounds irrespective of layer acidity. The spatial arrangements of organic compound were dependent on the relative strength between van der Waals interaction and hydrogen bonding. The Al_{13} was also introduced into the interlayer by using preswelled OALTN. The Al_{13}-PM was more stable than OALTN up to 400 °C for prolonged thermal treatment. Finally, the surface area of the Al_{13}-PM annealed at 400 °C was higher than that of the $KCa_2Nb_3O_{10}$-based pillared materials, but is rather small.

References

1. Clearfield, A. *Chem. Rev.* **1988**, *331*, 698.
2. Tang, X.; Xu, W.-Q.; Shen, Y.-F.; Suib, S. L. *Chem. Mater.* **1995**, *7*, 102.
3. Kim, R. M.; Pillion, J. E.; Burwell, D. A.; Groves, J. T.; Thompson, M. E. I. *Inorg. Chem.* **1993**, *32*, 4509.
4. Cheng, S.; Wang, T.-C. *Inorg. Chem.* **1989**, *28*, 1283.
5. Hou, W.; Yan, Q.; Fu, X. *J. Chem. Soc., Chem. Commum.* **1995**, *7*, 102.
6. Anderson, M. W.; Klinowski *Inorg. Chem.* **1990**, *29*, 3969.
7. Landis, M. E.; Aufdembrik, B. A.; Chu, P.; Johnson, I. D.; Kirker, G. W.; Rubin, M. K. *J. Amer. Chem. Soc.* **1991**, *113*, 3189.
8. Chen, Y.; Hou, W.; Guo, C.; Yan, Q.; Chen, Y. *J. Chem. Soc., Dalton Trans.* **1997**, 359.
9. Dion, M.; Ganne, M.; Tournoux, M. *Mat. Res. Bull.* **1981**, *16*, 1429.
10. Jacobson, A. J.; Johnson, J. W.; Lewandowwski, J. T. *Inorg. Chem.* **1985**, *24*, 3727.
11. Subramanian, M. A.; Gopalakrishnan, J.; Sleight, A. W. *Mater. Res. Bull.* **1988**, *23*, 837.
12. Uma, S.; Gopalakrishnan, J. *Chem. Mater.* **1994**, *7*, 6.
13. Gopalakrishnan, J.; Uma, S.; Bhat, V. *Chem. Mater.* **1993**, *5*, 132.
14. Hong, Y.-S.; Kim, S.-J. *Bull. Korean Chem. Soc.* **1996**, *17*(8), 730.
15. Mohan Ram, R. A.; Clearfield, A. *J. Solid State Chem.* **1991**, *45*, 94.
16. Hardin, S.; Hay, D.; Millikan, M.; Sanders, J. V.; Turney, T. W. *Chem. Mater.* **1991**, *3*, 977.
17. Akitt, J. W.; Elders, J. M.; Latellier, P. *J. Chem. Soc., Faraday Trans.* **1987**, *83*, 1725.
18. Hou, W.; Peng, B.; Yan, Q.; Fu, X.; Shi, G. *J. Chem. Soc., Chem. Commun.* **1993**, 253.
19. Sasaki, T.; Izumi, F.; Watanabe, M. *Chem. Mater.* **1996**, *8*, 777.
20. Setter, N.; Cross, L. E. *J. Mater. Sci.* **1980**, *15*, 2478.
21. Whittingham, M. S.; Jacobson, A. J. Intercalation Chem-

istry, Academic Press, New York, U. S. A., 1982.
22. Jacobson, A. J.; Johnson, J. W.; Lewandowski, J. T. *Mater. Res. Bull.* **1987**, *22*, 45
23. Clearfield, A.; Roberts, B. D. *Inorg. Chem.* **1988**, *28*, 3237.
24. Interrante, L. V.; Casper, L. A.; Ellis, A, N. Materials Chemistry, American Chemical Society, Washington D. C., 1995.

Temperature-Dependent Redox Isomerism *via* Intramolecular Electron Transfer. Synthesis and Properties of $Co(dmppz)_2(3,6\text{-}dbq)_2$ (dmppz=1,4-dimethylpiperazine; 3,6-dbq=3,6-di-*tert*-butyl-1,2-quinone)

Ok-Sang Jung*, Du Hwan Jo, Sung Ho Park, and Youn Soo Sohn

Inorganic Chemistry Laboratory, Korea Institute of Science and Technology, Seoul 136-791, Korea
Received March 15, 1997

The preparation and characterization of $Co(dmppz)_2(3,6\text{-}dbq)_2$ (dmppz=1,4-dimethylpiperazine; 3,6-dbq=3,6-di-*tert*-butyl-1,2-quinone) are established. Temperature-dependent magnetic moments (100-400 K), variable-temperature IR, and electronic spectra are presented to show that the title complex exhibits an equilibrium *via* a catechol to cobalt intramolecular electron transfer. At temperatures below 350 K, the charge distribution of the complex is $Co^{III}(dmppz)_2(3,6\text{-}dbsq)(3,6\text{-}dbcat)$ (3,6-dbsq=3,6-di-*tert*-butyl-1,2-semiquinonato; 3,6-dbcat=3,6-di-*tert*-butylcatecholato) whereas at the temperature beyond 390 K, the complex is predominantly $Co^{II}(dmppz)_2(3,6\text{-}dbsq)_2$ form in the solid state. At the temperature range of 350-390 K a mixture of Co(III) and Co(II) redox isomers exist at equilibrium. The transition temperature (Tc) of Co(III)/Co(II) in solution is approximately 50° lower than that in the solid state. In particular, thermal analysis on solid sample of the complex discloses that the transition for the Co(III)/Co(II) is accompanied by the change in heat content of 12.30 kcal/mol.

Introduction

The striking facet of the challanging issues in molecular chemistry deals with the use of molecular compounds in electronic devices and systems.[1-3] Small collections of these molecules could be expected to exhibit bistability which can be switched from one state to another by an external perturbation.[4-10] For instance, structural changes that accompany shifts in metal oxidation state have been applied to materials that exhibit photomechanical and optical switching signal creating an addressable memory effect. Charge transfer, *cis-trans* isomerism, proton transfer, and *etc.* have been investigated for some molecules with either structural mobility or chemical sensitivity.[11-13] Among the various systems, coordination metal complexes that exhibit intramolecular electron transfer phenomena have been the subjects of most intense study.

One of the most intriguing aspects of transition metal complexes containing 1,2-semiquinone (sq) and catechol (cat)[14] ligands is a unique facility for intramolecular electron transfer between the metal and chelated catechol ligands. This has been most prominently illustrated for the cobalt complexes, $Co^{III}(N\text{-}N)(sq)(cat)$ where temperature- or photo-induced equilibria between the following redox isomers have been observed in solution and in the solid state (1).[15,16] One isomer consists of Co(III) with one semiquinonate and one catecholate ligand and a diimine ligand, and the other

$$Co^{III}(N\text{-}N)(sq)(cat) \rightleftharpoons Co^{II}(N\text{-}N)(sq)_2 \qquad (1)$$

of Co(II) with two semiquinonate ligands and a diimine ligand. The intramolecular electron transfer is a consequence of charge localization within the molecule and the close energy separation between localized quinone and metal electronic levels. In particular, an intense band near 2500 nm (4000 cm^{-1}) assigned as cat to Co(III) charge transfer has been characteristically observed for Co(III) forms.[17-20] Moreover, for such complexes, the bistability and its Tc have been elucidated to be very sensitive to the nature of the diimine coligands.[20] In the present report, we describe the synthesis and characteristic properties of the $Co(dmppz)_2(3,6\text{-}dbq)_2$ based on spectroscopic, magnetic, and thermal analyses. The physicochemical properties induced by the bistability of the complex is primarily discussed.

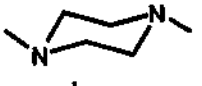

dmppz

Experimental

Materials and Instrumentation. Dicobaltoctacarbonyl ($Co_2(CO)_8$) and 1,4-dimethylpiperazine (dmppz) were purchased from Strem and Aldrich, respectively. 3,6-Di-*tert*-butyl-1,2-benzoquinone (3,6-dbbq) was prepared according to literature procedure.[21] Elemental analysis (C,H,N) was carried out at the Korea Basic Science Center. Infrared spectra were obtained in 5000-400 cm^{-1} range on a Perkin Elmer 16F PC FTIR spectrophotometer with sample prepared as